

1 **Proposal of a new empirical model with flow velocity to improve time-**
2 **weighted average concentration estimates from the Polar Organic Chemical**
3 **Integrative Samplers**

4
5 Nicolas Mazzella ^{a,*}, Marion Bernard ^a, Robin Guibal ^b, Sebastien Boutry ^a, Sophie Lissalde ^b,
6 Gilles Guibaud ^b

7
8 ^a INRAE, UR EABX, 50 Avenue de Verdun, 33612 Cestas, France

9 ^b Université de Limoges, E2Lim, 123 Avenue Albert Thomas, Limoges, Cedex 87060, France

10 * Corresponding author at: INRAE, UR EABX, 50 Avenue de Verdun, 33612 Cestas, France

11 **E-mail address:** nicolas.mazzella@inrae.fr

12
13 **Abstract**

14
15 It is now widely recognized that the sampling rate of Polar Organic Chemical Integrative
16 Samplers (POCIS) is significantly affected by flow velocity, which can cause a consequent bias
17 when determining time-weighted average concentrations (TWAC). We already observed the
18 desorption of deisopropylatrazine (DIA) over time when added to the receiving phase of a
19 POCIS. This desorption rate was particularly influenced by flow velocity, in an agitated water
20 environment *in situ*. In the method presented here, we calibrated 30 pesticides under controlled
21 laboratory conditions, varying the flow velocity over four levels. We simultaneously studied
22 the desorption rate of DIA-d5 (a deuterated form of DIA) over time. An empirical model based
23 on a power law involving flow velocity was used to process the information from the
24 accumulation kinetics of the compounds of interest and elimination of DIA-d5. This type of
25 model makes it possible to consider the effect of this crucial factor on exchange kinetics, and
26 then to obtain more accurate TWACs with reduced bias and more acceptable dispersion of
27 results.

28
29 **Keywords**

30 Passive sampling, pesticides, sampling rates, calibration, kinetic model, accuracy.

31

32 1. Introduction

33 Sampling rate (R_s) is a critical parameter when using passive samplers to estimate a
34 time-weighted average concentration (TWAC). R_s can be represented by the volume of water
35 purified by a passive sampler per unit time for a given compound (Alvarez et al. 2004). This
36 parameter must be determined in a prior calibration step. However, transferring such sampling
37 rates to the field can lead to uncertainties about the results because experimental conditions in
38 the laboratory generally differ from those in the field. Indeed, R_s depends on a number of
39 environmental factors such as turbulence, temperature, salinity, organic and suspended matter
40 content, and biofouling (Söderström et al. 2009, Vrana et al. 2005). Among these factors, flow
41 velocity is known to play a key role in water boundary layer thickness, which can cause the
42 associated sampling rate to vary quite significantly, resulting in large biases up to factors of 3–
43 4 (Mazzella et al. 2010). Recently, diffusive passive samplers have been developed to overcome
44 the effects of flow velocity on the uptake of chemicals, including the technologies organic
45 Diffusive Gradients in Thin-films (o-DGT) and Microporous Polyethylene Tube (MPT)
46 (Fauvelle et al. 2017b, Guibal et al. 2019). In these cases, the strategy consists in increasing the
47 membrane resistance to limit the consideration of the water boundary layer (WBL) thickness
48 relative to the flow velocity variations. This approach is however limited at very low flow
49 velocities ($\approx 1 \text{ cm s}^{-1}$) (Fauvelle et al. 2017a) or, for o-DGT, requires different diffusion gel
50 thicknesses to explicitly evaluate the WBL contribution (Bonnaud et al. 2023, Bonnaud et al.
51 2022, Challis et al. 2016). With a Polar Organic Chemical Integrative Sampler (POCIS)
52 configuration, another solution for correcting such flow velocity induced biases is Performance
53 Reference Compounds (PRCs). The rate of desorption (k_e) of a PRC relative to the flow velocity
54 must be correlated with the simultaneous uptake of the pollutant(s). This is equivalent to
55 assuming that the exchanges within the sampler are isotropic, regardless of the compound of
56 interest. An $R_s \text{ in situ}$ can then be estimated for each molecule by extrapolating the k_e of the PRC
57 observed under given flow conditions. The correction factor, known as the environmental
58 adjustment factor (EAF), can then be determined from the ratio of k_e obtained in the laboratory
59 ($k_e \text{ calibration}$) and in the field ($k_e \text{ in situ}$).

60 For POCIS, we previously showed that desisopropylatrazine-d5 (DIA-d5) had a
61 satisfactory desorption potential and checked the isotropy for this single compound (Mazzella
62 et al. 2007). The application of an EAF made it possible to obtain quite accurate field estimates
63 of $R_s \text{ in situ}$ for some polar substances (Lissalde et al. 2011, Lissalde et al. 2014). However, this
64 empirical approach included phenomena of adsorption of molecules in the membrane

65 (Vermeirssen et al. 2012), their diffusion in the micro- and macroporosity of the receiving phase
66 and, finally, their binding to one of the two interaction sites (i.e., hydrophilic or hydrophobic)
67 within the same adsorbent (Bäuerlein et al. 2012). Furthermore, highly polar compounds that
68 can be desorbed and used as PRCs, and more hydrophobic molecules that are more strongly
69 retained in the receiving phase, are likely to be influenced in different ways by all of these
70 processes (Harman et al. 2011). As a result, while the PRC approach with an EAF correction
71 provided satisfactory results for POCIS with some triazine, phenylurea, and chloroacetanilide
72 herbicides (Dalton et al. 2014, Lissalde et al. 2014, Mazzella et al. 2010), it has not yet been
73 possible to generalize it to other substances because we do not know enough about the
74 mechanisms at work. The approach also requires compliance with the “80/20 rule” (Booij and
75 Smedes 2010). In other words, the PRC desorption rate after field exposure must be between
76 20 and 80% of the initial content of this compound, when the receiving phase is spiked. Thus,
77 if the PRC used has very little desorbed (i.e., residuals after exposure >80%) or, on the contrary,
78 has been completely eliminated (i.e., residuals after exposure <20%), then we cannot apply the
79 EAF-based method. Nevertheless, these are only the most severe and problematic cases of bias,
80 indicating that flow velocity was either extremely low or much greater than in the laboratory,
81 during both calibration and R_s determination steps.

82 In this study, a POCIS calibration was performed with some selected moderately polar
83 pesticides (i.e., $\log K_{ow}$ between 2 and 4) according to increasing flow velocities. The
84 relationship between sampling rates and simultaneous desorption rate of DIA-d5 was
85 investigated using a power-law relationship with water flow velocity as parameter. Based on
86 these findings, we propose a model that accounts for the effects of such a factor more explicitly.
87 We assessed the improvements offered by this new method by using it to reprocess previous
88 data. It avoids, for instance, the main limitations of the earlier EAF approach (i.e., the unproven
89 hypothesis of isotropic exchange for all analytes and the “80/20 rule” constraint). In addition,
90 it appears possible to obtain a lower confidence interval associated with the variability of R_s as
91 a function of the estimated flow rate, now ranging from 47 to 61%, compared with the over
92 200% previously obtained empirically.

93

94

95 2. Material and methods

97 2.1. Chemicals and reagents

98 The solvents (methanol, acetonitrile and ethyl acetate – HPLC grade) were obtained
99 from Biosolve (Biosolve SARL, Dieuze, France). Ammonium acetate was purchased from
100 Fluka (Sigma Aldrich, Schnellendorf, Germany). Ultrapure water (UPW, resistivity > 18 MΩ)
101 was produced by a Synergy UV system from Millipore (Billerica, MA, USA). Analytical
102 standards, DIA-d5 and internal standards (atrazine-d5, carbofuran-d3, DEA-d6, diuron-d6,
103 methomyl-d3, metolachlor-d6, pyrimicarb-d6 and tebuconazol-d6) of >95.5% purity were
104 purchased from Dr. Ehrenstorfer GmbH (Augsburg, Germany). Individual stock solutions were
105 prepared in acetonitrile (100 mg L⁻¹) and stored at -18°C for no more than six months. A
106 working solution containing each of the analytical standards was prepared by dilution of the
107 individual stock solutions in acetonitrile (1 mg L⁻¹). This was stored at -18°C for six months.

108 2.2. Sampler preparation and analysis

109 The passive sampler configuration used was a POCIS (Alvarez, 2004) containing 200
110 mg of Oasis® HLB sorbent (30-µm particle size, 810 m² g⁻¹, divinylbenzene-N-
111 vinylpyrrolidone, Waters, France) sandwiched between two microporous polyethersulfone
112 membranes of 90 mm diameter and 0.1 µm pore size (PALL®, VWR, France). Two support
113 stainless discs were used to maintain the membrane-sorbent-membrane layers (inner diameter
114 5.4 cm, outer diameter 10.2 cm). Prior to assembling the POCIS device, the Oasis® HLB
115 sorbent was spiked with DIA-d5 at approximately 4 µg g⁻¹ (Mazzella et al. 2010), with methanol
116 as the spiking diluent (Belles et al. 2014). Each spiked POCIS exposed during the calibration
117 step was associated with a triplicate of “references” (3 mL empty polypropylene SPE tubes and
118 polyethylene frits containing the same sorbent). These references were used to determine both
119 the initial spike concentration ($C_{(0)}$) and homogeneity. After exposure, the POCIS were kept at
120 4°C for 24 h, then treated and analyzed with the references by HPLC-ESI-MS/MS as described
121 in previous studies (Bernard et al. 2022, Lissalde et al. 2011). Briefly, quantitations were done
122 using internal calibration curves ranging from 1 to 100 µg L⁻¹. For quality assurance and quality
123 control, procedural blanks and two calibration points (i.e., 5 and 25 µg L⁻¹) were periodically
124 injected every 10 samples. In addition, recoveries from spiked POCIS were checked and
125 typically observed to be between 80 ± 20%, as reported in earlier studies (Lissalde et al. 2011,
126 Mazzella et al. 2007).

2.3. Calibration of POCIS under different flow velocities

To calculate average concentrations in the aquatic environment from those measured in the POCIS HLB receiving phase, one must determine the accumulation kinetic constants associated with each target substance. To do this, POCIS were exposed in channels filled with tap water (500 L) initially spiked with a selection of contaminants at a concentration of $0.5 \mu\text{g L}^{-1}$ (see list of analytes in Table 1). Then, 14 POCIS were exposed to the following flow velocities: $V1 = 2.7 \pm 0.9 \text{ cm s}^{-1}$; $V2 = 7.2 \pm 1.0 \text{ cm s}^{-1}$; $V3 = 19.9 \pm 3.3 \text{ cm s}^{-1}$. To maintain contaminant concentration constant in the medium over the 21 days of calibration, a daily renewal rate of 15% of the water volume was applied using multi-channel peristaltic pumps (75 L d^{-1}). To compensate for this renewal and maintain the pesticides at a nominal concentration around $0.2 \mu\text{g L}^{-1}$ (data are provided in an Excel file in the supp. mat.), a constant supply of contaminants was provided by a syringe pump containing the spiking solution (10 mg L^{-1}), at a flow rate of 3 mL d^{-1} . A 100-L tank, subject to the same spiking and renewal conditions as the channels, was used to expose the POCIS to near-zero flow velocity: $V0 = 0.3 \pm 0.2 \text{ cm.s}^{-1}$ (Figure S 1). Further details on the experimental setup can be found in Guibal et al. (Guibal et al. 2020). The POCIS were removed in duplicate at different times (1, 3, 5, 7, 10, 15, and 21 days), and replaced with “blanks” (i.e., non-analyzed POCIS) to maintain a consistent sampling pressure on the experimental system. Regular ($t = 0, 2, 5, 7, 12, 14, 16, 19, \text{ and } 21$ days) water sampling was carried out to monitor channel concentration over the 21-day calibration period. Analyses of both POCIS and spot water samples were performed by HPLC-MS/MS as described elsewhere (Lissalde et al. 2011). POCIS extracts were typically diluted 1:3 prior to analyses.

For each flow velocity, the kinetic constants were determined by plotting the concentration factor ($CF_{HLB}, \text{ L g}^{-1}$) against time (d), where CF_{HLB} is determined with Equation 1:

$$\text{Equation 1} \quad CF_{HLB} = \frac{C_{POCIS}}{C_{w \text{ weighted}}}$$

where C_{POCIS} is the amount of analyte trapped in the POCIS phase ($\mu\text{g g}^{-1}$), and $C_{w \text{ weighted}}$ concentration in water ($\mu\text{g L}^{-1}$) corresponds to POCIS exposure time as in previous studies (Bernard et al. 2022, Fauvelle et al. 2012, Lissalde et al. 2011, Mazzella et al. 2007). $C_{w \text{ weighted}}$ over consecutive periods (i.e., 0–2 d, 2–12 d or 0–21 d) are provided as supplementary material (SI_accumulation and water conc. Excel file).

157 If the analyte follows linear accumulation kinetics (Figure S 2), a linear model (LM) can be
158 used to determine the kinetic constants as follows:

159 Equation 2 $CF_{HLB} = k_u \cdot t = \frac{R_s \cdot t}{M_{POCIS}}$

160 where k_u is the kinetic constant for analyte uptake ($L d^{-1} g^{-1}$), t the exposure time (d), R_s the
161 sampling rate in $L d^{-1}$, and M_{POCIS} the mass of HLB sorbent (g) in the POCIS.

162 For DIA-d5, which we used as a performance reference compound, the analyte followed first-
163 order elimination kinetics, and a nonlinear least-squares model (NLS) can be used to determine
164 the kinetic constants as follows:

165 Equation 3 $C_{(t)} = C_{(0)} \cdot e^{-k_e t}$

166 where $C_{(t)}$ is the concentration of PRC measured in the HLB sorbent after an exposure time t ,
167 and $C_{(0)}$ the initial concentration of DIA-d5 within the same sorbent. From this relationship, we
168 can then deduce the exchange constant k_e (d^{-1}).

169 2.4. Theory and modeling

170 In the previous studies (Booij et al. 2020, Vermeirssen et al. 2012), flow effects on R_s
171 were empirically modeled by a power-law relationship with flow velocity as follows:

172 Equation 4 $R_s = b \cdot U^m + c$

173 Furthermore, the sum of the resistances for transport through the water boundary layer (WBL),
174 membrane and sorbent equals the overall resistance to mass transfer ($1/k_o$) (Alvarez et al. 2007,
175 Fauvelle et al. 2017a):

176 Equation 5 $\frac{1}{k_o} = \frac{A}{R_s} = \frac{1}{k_w} + \frac{A}{R_{s,max}}$

177 where $1/k_w$ is the resistance associated with the WBL thickness of the water-membrane interface
178 and $A/R_{s,max}$ is the residual resistance (i.e., $1/k_w \rightarrow 0$) associated with the membrane thickness
179 and/or the diffusion in the interstitial water surrounding the sorbent particles. A corresponds to
180 the effective exchanging surface area of a POCIS. This value was previously found to be
181 between 11.2 and 16.9 cm^2 depending on the sorbent mass used as the receiving phase (Fauvelle
182 et al. 2014). In fact, when the device is immersed and the receiving phase is fully wetted the

183 sorbent is seen to rapidly sink to the bottom of the POCIS. This generally results in a smaller
184 effective surface area than expected as the sorbent then only covers one third of the total
185 membrane surface area. Thus, in the present study, an average value of $A = 15 \text{ cm}^2$ (average
186 value typically observed in our laboratory when calibrating POCIS with 5.4 cm inner diameter
187 and 200 mg of receiving phase) was systematically considered.

188 For the method proposed here, we adopted a similar approach to the previous studies
189 mentioned, while taking into account the mass transfer resistance, $1/k_o$ (d cm^{-1}) during the
190 uptake regime for chemicals that we calibrated at different flow velocities (U ; cm s^{-1}). If we
191 also consider $m \approx 0.5$, as suggested by Booij and Chen (Booij and Chen 2018) for atrazine
192 uptake with POCIS, we can obtain the following model:

193 Equation 6
$$\frac{1}{k_o} = \frac{b}{\sqrt{U}} + c$$

194 where b and c are expressed in $\text{d cm}^{-1/2} \text{ s}^{-1/2}$ and d cm^{-1} , respectively.

195

196 3. Results and discussion

197

198 3.1. Nonlinear modeling for flow velocity-mass transfer relationships

199 As shown in Figure 1 (a), the fitting of Equation 6 considering all the R_s data results in
200 a power-law curve indicating a rapid decrease of the resistance as the flow velocity increases.
201 The b and c parameters adjusted for all substances are given in Table 1. It is also possible to fit
202 a more general curve considering all 92 observations, including every compound, and thus to
203 obtain the global parameters $b = 0.100 \pm 0.002$ and $c = 0.019 \pm 0.004$. The quality of this global
204 fit can be judged by the $R^2 = 0.967$ and distribution of the residuals, which appears acceptable
205 (Figure S 3). The residuals are, on the whole, rather uniformly distributed around zero.
206 However, there is some heteroscedasticity with the dispersion of the residuals increasing for
207 V_0 . This can be explained by the higher uncertainty in the estimation of R_s , which was then
208 used to derive $1/k_o$, due to the boundary layer control when the flow velocity is very low. In
209 other words, in this particular condition, in Equation 5, the $1/k_w$ term predominates over the
210 $A/R_{s,max}$ term, reflecting a stronger influence of the WBL (and the diffusion of the compounds
211 in it) as U decreases. Conversely, for $U \rightarrow \infty$, the $1/k_w$ term becomes almost negligible and the
212 contribution of $A/R_{s,max}$ is more likely to be estimated. Finally, for all observations, five values
213 lie outside the ± 2 standard deviation interval typically representing a 95 % confidence interval.

214 Lissalde et al. (2014) observed that *in situ* k_e of DIA-d5 (Equation 3) increased with
215 increasing flow velocity. In such a desorption regime (i.e., DIA-d5), we obtain a rewriting of
216 Equation 6 as follows:

$$217 \text{ Equation 7 } \frac{1}{k_{o(DIA-d5)}} = \frac{A}{K_{sw} \cdot M_{POCIS} \cdot k_e} = \frac{b_{(DIA-d5)}}{\sqrt{U}} + C_{(DIA-d5)}$$

218 where K_{sw} corresponds to the HLB-water sorption coefficient in the case of DIA uptake. During
219 the calibration, the uptake of the DIA followed nonlinear kinetics, as previously observed
220 (Bernard et al. 2022, Fauvelle et al. 2012, Mazzella et al. 2007), and an average value of $K_{sw} =$
221 $30370 \pm 3600 \text{ mL g}^{-1}$ was observed (raw data are provided in an Excel file in the supp. mat.).
222 In the same way as with the uptake data of the calibrated compounds (see above), when the
223 desorption of DIA-d5 was treated with Equation 7, it produced the curve shown the Figure 1
224 (b). The corresponding coefficients b and c for DIA-d5 are reported at the bottom of Table 1.

225 Another way of representing modeling of this kind (Equation 6 or its application to DIA-
226 d5 only in Equation 7) is to transform the x and y values into a logarithmic scale. For example,
227 by considering $\log_{0.5}$ for the flow velocity because this factor evolves according to its square
228 root, and, in a more conventional way, the decimal log of $1/k_0$. In this case, we obtain a linear
229 form described by Equation 8 (Figure S 4). This leads to the same estimations of coefficients b
230 and c , but with the benefit of making an F-test possible (Table S 2) to check whether the
231 variance is due to the model fitting or experimental random error.

232 Equation 8
$$\log_{10}\left(\frac{1}{k_0}\right) = b_1 \times \log_{0.5}(U) + C_1$$

233 In this relationship, parameters b_1 and c_1 differ from b and c defined earlier because the variables
234 underwent a logarithmic transformation.

235 A practical limitation of the PRC approach with POCIS has generally been reported
236 because of the "80/20 rule". For instance, Buzier et al. (2019) mention that PRC correction
237 efficiency increased with the deployment time, but significant desorption of DIA-d5 was
238 observed under quiescent conditions during at least 15 and 21 days of exposure. Other
239 compounds, such as cyanazine, have been studied as PRCs (Belles et al. 2014). Although the
240 elimination rates of cyanazine and DIA were different in this earlier study, flow velocity
241 appeared affect both in the same way. The authors concluded that, given their different
242 desorption rates, it would be possible to use these two compounds as PRCs simultaneously,
243 particularly by applying a model based on an environmental adjustment factor (Equation 9).
244 The latter necessarily requires compliance with the "80/20 rule". In practice, one of the two
245 PRCs would have completely desorbed, and thus be unusable, while the other one would lose
246 between 20 and 80% of its initial quantity. The model we propose is fitted with the desorption
247 of DIA-d5, although a similar approach with another PRC, such as cyanazine, would probably
248 result in an analogous outcome (i.e., the resistance to mass transfer would drop with the velocity
249 of flow according to a power-law relationship). Actually, in the model proposed here, this
250 restriction (i.e., the need for a PRC desorption rate > 20%) is no longer required. In the specific
251 case where $C(t) \approx C(0)$ (and then $k_e \rightarrow 0$; Equation 3) after a given period of *in situ* deployment
252 (typically ≥ 2 weeks), we would then have an estimate of $U < 1 \text{ cm s}^{-1}$ (application of Equation
253 7). The resulting R_s estimates for the analytes of interest would be close to the minimum, i.e.,
254 around 100 mL d^{-1} . Such estimates would be considerably lower than R_s values typically
255 obtained during laboratory calibration (usually $200\text{--}400 \text{ mL d}^{-1}$), with a U between 2 to 10 cm

256 s^{-1} (Ahrens et al. 2015, Bernard et al. 2023, Fauvelle et al. 2012, Lissalde et al. 2011, Morin et
257 al. 2013, Morin et al. 2018, Poulier et al. 2014).

258 Equation 9
$$R_{s-analyte (in situ)} = \frac{R_{s-analyte (calibration)}}{k_{e-PRC (calibration)}} \times k_{e-PRC (in situ)}$$

259 Figure 2 shows that b and c values are unlikely to follow a normal distribution. We
260 therefore plotted the medians in red together with their percentiles, covering 65% of the data
261 (equivalent to ± 1 standard deviation), and then 95% of the data. Looking first at the values in
262 the red areas only, we see a dispersion of b accordingly to the 95% percentiles, ranging from
263 0.07 to 0.46 around a median of $0.127 \text{ d cm}^{-1/2} \text{ s}^{-1/2}$. If we consider 65% of the data, the range
264 is indeed narrower, between 0.08 and $0.23 \text{ d cm}^{-1/2} \text{ s}^{-1/2}$, revealing the higher deviations for the
265 compounds fluzilazole, boscalid, chlorfenvinphos and linuron. In other words, most of the
266 analytes have b parameters that converge towards the central value defined by the median. The
267 mean was also fairly close, estimated at $0.161 \text{ d cm}^{-1/2} \text{ s}^{-1/2}$. For the c parameter, and again for
268 the values delimited by the red areas, the dispersion around the median (0.005 d cm^{-1}) appeared
269 to be higher, even when only 65% of the data were considered ($0.000\text{--}0.018 \text{ d cm}^{-1}$). This is
270 primarily because many estimates of the c parameter tended towards 0 (11 compounds out of
271 30) after applying Equation 6 modeling. However, the mean of c (0.008 d cm^{-1}) remained close
272 to the median, and of the same order of magnitude.

273 In summary, for the majority of the analytes studied here, it might be feasible to estimate
274 parameters b and c through the use of values that fall around the median (or mean). Considering
275 such "generic" constants for b and c , an attempt would then be made to pinpoint the degree of
276 error and specific potential biases that may result.

277 3.2. Model output and validation steps

278 We calculated flow velocity ($U_{calculated}$) from the elimination rate of DIA-d5 using
279 Equation 7. This flow velocity estimate was then used to calculate $k_o_{calculated}$ (Equation 6).
280 Finally, R_s was deduced by multiplying $k_o_{calculated}$ with effective surface area (i.e., 15 cm^2). In
281 Figure 3, we plotted the $1/k_o$ obtained experimentally during calibration under quiescent
282 conditions (i.e., V0) against the $1/k_o_{calculated}$ from the DIA-d5 elimination rate. The alignment
283 on the $y = x$ line, and fact that all projected points are within the $\pm 20\%$ interval, indicate a good
284 equivalence between the $1/k_o$ data obtained with the two approaches. The same exercise can be
285 carried out for the highest flow velocity applied during POCIS calibration (i.e., V3). Figure 4
286 (a) shows a similar comparison and agreement between experimental and recalculated $1/k_o$,

287 although there are significant deviations for fluzilazole, boscalid, chlorfenvinphos and linuron
288 in this case. It is also noteworthy that flusilazole, boscalid, chlorfenvinphos and linuron have
289 higher b values than the other compounds (Table 1 and Figure 2). It is expected that b is fairly
290 independent of compound, since k_w increases only weakly with increasing D_w , as reported by
291 Booij and Chen (2018) in the case of atrazine sampling by POCIS. For these four chemicals, a
292 significant bias of about +82% may appear at high flow rates $\geq 20 \text{ cm s}^{-1}$. With the exception
293 of linuron, these are among the most hydrophobic compounds on the list, with $\log K_{ow}$ between
294 3.8 and 4.9. Based on the compounds calibrated here, it is therefore possible that this approach
295 is limited to moderately polar chemicals with $\log K_{ow}$ essentially between 2.1 and 3.8 (Table
296 1). Such a result seems to be supported by the results of a two-way ANOVA (Table S 1),
297 considering the factors D_w (i.e., diffusion in water at 25°C) and $\log K_{ow}$. This analysis revealed
298 that coefficient c , which could be associated with diffusion across the membrane, may partly
299 depend on $\log K_{ow}$. However, unlike for passive samplers dedicated to hydrophobic compounds,
300 K_{ow} alone remains a poor predictor of K_{sw} and K_{mw} for passive samplers with hydrophilic
301 microporous membranes and sorbent (Bonnaud et al. 2023). The difference could indicate that
302 this type of analyte may interact with the membrane matrix or surface during transfer through
303 the water-filled pores. In other words, the porous media mass transport equations proposed by
304 Booij et al. (2017) are probably unsuitable for such chemicals, unlike atrazine ($\log K_{ow}$
305 estimated at 2.6).

306 Parts (b) and (c) of Figure 4 summarize the distribution of experimental and recalculated
307 R_s for the two boundary flowing conditions (i.e., V0 and V3). It appears that both types of R_s
308 values would be around 75 mL d^{-1} for a quiescent medium (and vary between 30 and 120 mL
309 d^{-1} according to the observation confidence interval), regardless of the diffusion in water (D_w)
310 or polarity ($\log K_{ow}$) of the substances considered (Table 1). The same appears to be valid for a
311 highly agitated medium, with a mean R_s of 400 mL d^{-1} (varying between 200 and 600 mL d^{-1}
312 according to the observation confidence interval). Consequently, for a flow velocity very close
313 to zero, we can assume that the sampling rates can vary around a central value with a dispersion
314 of $\pm 61 \%$ (implying a relative standard deviation of about 30.5 % and with a t-value of 2 for a
315 confidence interval of 95 %). The resulting enlargement for the relative standard deviation of
316 R_s (i.e. 61%) seems significantly lower than what we were able to ascertain empirically by
317 Poulier et al. (2014). Actually, in this earlier study, an enlargement factor of two-folds (i.e. from
318 -50% to +100% R_s amplitude) was typically used with an R_s obtained from laboratory
319 calibration to extrapolate to field conditions with different flow regimes.

320 We applied our approach to previously published laboratory and *in situ* calibration data.
321 Table 2 shows the current velocities ($U_{\text{estimated}}$) recalculated using Equation 7 and the
322 coefficients from Table 1, as well as the k_e reported for DIA-d5 in these previous studies. The
323 resulting recalculated flow velocities were in good agreement with the values previously
324 measured (U_{measured}) with an electromagnetic flow meter. Table 3 shows the R_s estimated for
325 some pesticides (with $\log K_{ow}$ between 2.5 and 3.5, and a mean $\log K_{ow}$ of 3.125) using Equation
326 6 and the parameters b and c from the present calibration. Under these conditions (i.e., a
327 “specific model”), an estimate of mean R_s of 308 mL d⁻¹ was obtained, for example, in contrast
328 to a mean R_s of 280 mL d⁻¹ determined experimentally elsewhere (Fauvelle et al. 2012) (i.e., a
329 relative deviation of 10% on average). A similar comparison with two other POCIS calibration
330 datasets (Lissalde et al. 2011, Mazzella et al. 2007) indicated a bias that is also fairly low,
331 ranging from 10 to 25%. A larger discrepancy can be observed in *in situ* data (70% bias), but
332 must be put into perspective considering that only atrazine was detected during this field study
333 (Mazzella et al. 2010). The exercise was also carried out considering the “generic” coefficients
334 with $b' = 0.100 \text{ d cm}^{-1/2} \text{ s}^{-1/2}$ and $c' = 0.019 \text{ d cm}^{-1}$ (i.e., the “general model”), resulting in quite
335 acceptable deviations, rather close to the biases observed with the “specific models” fitted for
336 each compound reported here.

337 Finally, the previously defined median was in good agreement with the mean of $b' =$
338 0.100 ± 0.004 (95% confidence interval limits) when we plotted the values of the “generic” b'
339 and c' parameters on Figure 2 (dashed lines and blue areas). The discrepancy appears to be
340 larger for $c' = 0.019 \pm 0.008$, but the red area, which contains 95% of the c values, and the blue
341 area, which represents the confidence interval associated with the mean value of c' , overlap
342 significantly. This makes the differences non-significant, so parameters b' and c' could be used
343 when applying Equation 6 to estimate R_s , taking into account the influence of the current
344 velocity by the additional use of Equation 7. In this case, we would have to accept biases of 10
345 to 25% in stirred conditions (i.e., $> 2\text{--}3 \text{ cm s}^{-1}$) and up to 70% in quiescent conditions. In light
346 of this possibility, a template containing the two generic coefficients b' and c' is provided in the
347 supplementary material (see file “SI_Rs and Ksw data and template.xlsx”).

348

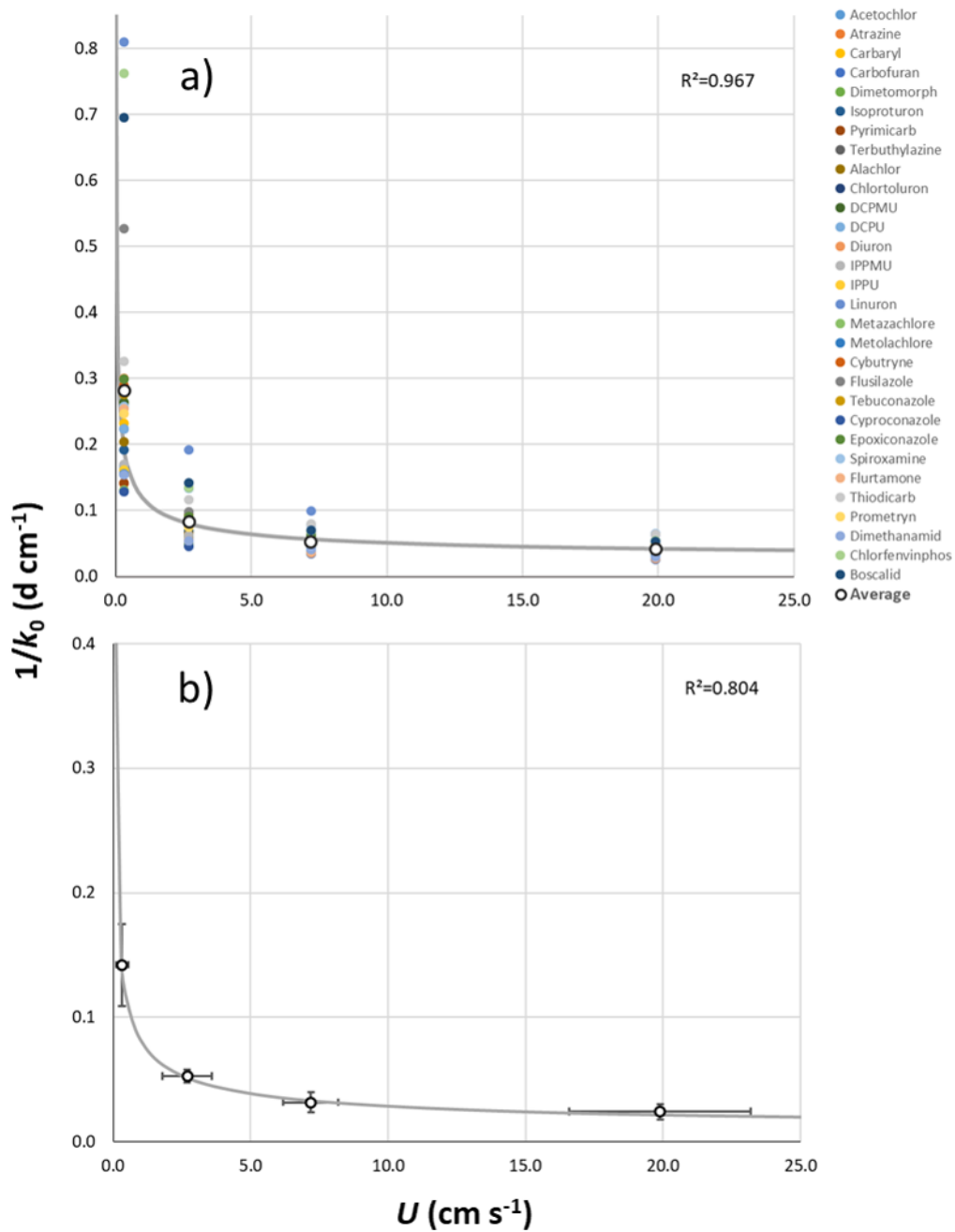
349

350 **4. Conclusion**

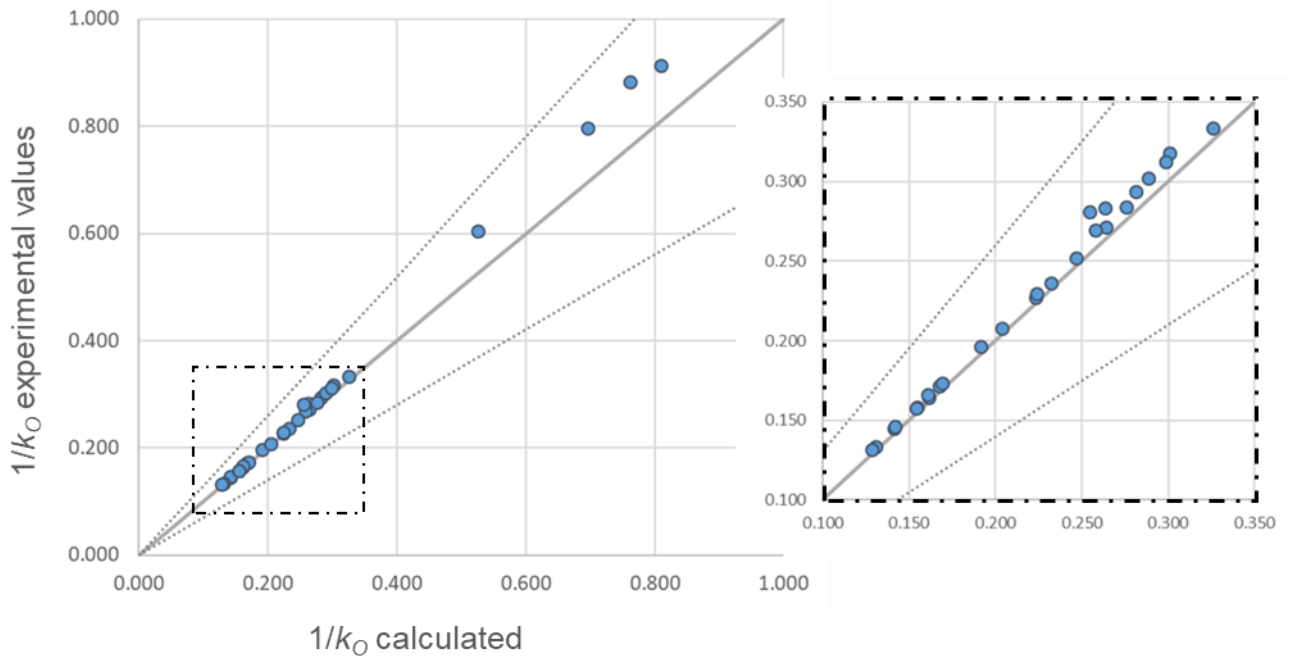
351 In this study, a POCIS calibration was performed with some moderately polar pesticides
352 (i.e., $\log K_{ow}$ between 2 and 4) as flow velocities increased. A power-law relationship with
353 water flow velocity as a parameter was used to investigate the relationship between sampling
354 rates and simultaneous desorption rate of DIA-d5. Based on these findings, we proposed a
355 model that explicitly accounts for the effects of such a factor. We evaluated the benefits of this
356 new method by reprocessing previous data with it. This approach also cuts out the main
357 limitations of the previous EAF approach, such as the unproven hypothesis of isotropic
358 exchange for all analytes and the "80/20 rule" constraint. Furthermore, it appears that a lower
359 confidence interval associated with the variability of R_s as a function of flow rate.

360

361



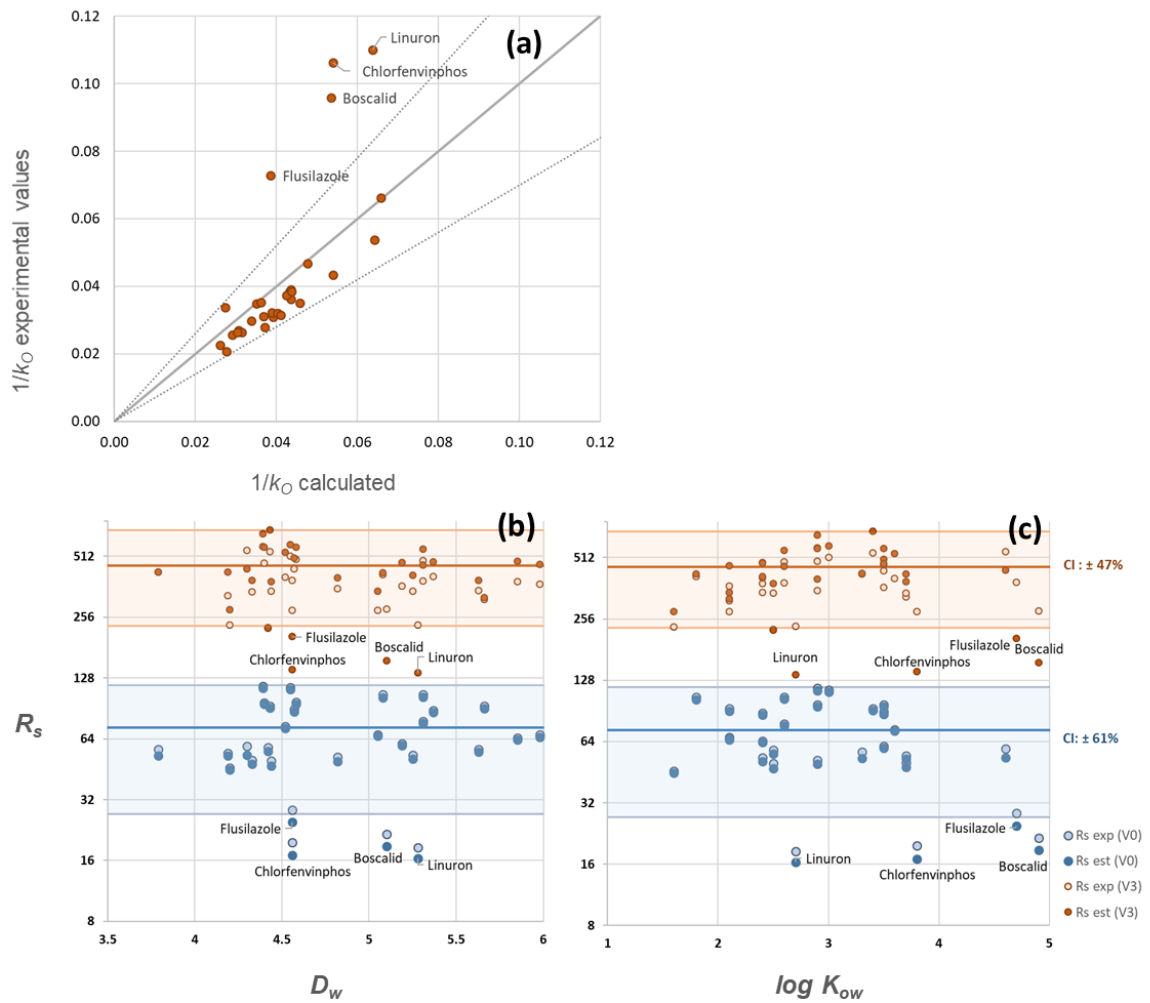
365 Figure 1. Variation of mass transfer resistance vs. flow velocity: a) for all chemicals during a
 366 linear uptake only, and the fitting of Equation 6 with average values, b) for DIA-d5 only
 367 during the desorption process (standard deviations on both $1/k_0$ estimates of DIA-d5 and the
 368 flow velocity measurements are reported in this lower panel).



377

378 Figure 3. Correlation ($y = x$ with $\pm 20\%$ interval limits indicated by the dotted lines) between
 379 $1/k_O$ experimental data (y-axis) at V_0 flow condition and $1/k_O$ recalculated estimates with
 380 Equation 6 (x-axis).

381



382

383 Figure 4. (a) Correlation ($y = x$ with $\pm 20\%$ interval limits indicated by the dotted lines) between
 384 $1/k_O$ experimental data (y-axis) at V3 flow condition and $1/k_O$ recalculated estimates with
 385 Equation 6 (x-axis). (b) R_s experimental and estimated data (V0 in blue and V3 in brown) as a
 386 function of D_w , (c) R_s experimental and estimated data (V0 in blue and V3 in brown) as a
 387 function of $\log K_{ow}$. Open and filled circles corresponds to experimental and estimated values,
 388 respectively. The brown and blue solid lines represent the mean values of the data, respectively.

389

390

391

392

393 Table 1. b ($\text{d cm}^{-1/2} \text{s}^{-1/2}$) and c (d cm^{-1}) parameters obtained for each compound following a
 394 linear uptake over 21 days, and R^2 of fitted linear models. b and c parameters deduced from
 395 DIA-d5 desorption curve are provided as well. The $\log K_{ow}$ and D_w values are also summarized.

Chemicals	b	c	R^2	RMSE*	$\log K_{ow}$ +	$D_w (\times 10^{-6} \text{ cm s}^{-1})$ §
Acetochlor	0.112 (0.006)	0.004 (0.005)	0.994	0.006	3.5	4.57
Atrazine	0.074 (0.002)	0.012 (0.002)	0.996	0.004	2.6	5.31
Carbaryl	0.128 (0.007)	0.004 (0.007)	0.980	0.015	2.4	5.85
Carbofuran	0.115 (0.005)	0.019 (0.005)	0.983	0.013	2.1	5.05
Dimetomorph	0.155 (0.009)	0.001 (0.000)	0.973	0.022	3.3	3.79
Isoproturon	0.102 (0.003)	0.011 (0.003)	0.992	0.008	2.6	5.31
Pyrimicarb	0.069 (0.001)	0.021 (0.001)	0.999	0.002	1.8	5.08
Therbuthylazine	0.090 (0.004)	0.002 (0.004)	0.979	0.011	3.4	4.43
Alachlor	0.088 (0.002)	0.011 (0.002)	0.985	0.012	3.6	4.52
Chlortoluron	0.161 (0.006)	0.001 (0.000)	0.988	0.015	2.4	5.25
DCPMU	0.145 (0.004)	0.008 (0.004)	0.996	0.008	2.1	5.63
DCPU	0.123 (0.004)	0.006 (0.004)	0.991	0.010	2.1	5.98
Diuron	0.174 (0.008)	0.001 (0.000)	0.990	0.015	2.5	4.44
IPPMU	0.089 (0.003)	0.013 (0.002)	0.992	0.007	2.4	5.37
IPPU	0.074 (0.003)	0.031 (0.003)	0.999	0.001	2.1	5.66
Linuron	0.502 (0.024)	0.000 (0.000)	0.987	0.049	3.0	5.28
Metazachlore	0.067 (0.002)	0.012 (0.002)	0.992	0.005	3.0	4.55
Metolachlore	0.082 (0.003)	0.009 (0.003)	0.986	0.008	3.5	4.40
Cybutryne	0.165 (0.008)	0.001 (0.000)	0.986	0.017	2.9	4.82
Flusilazole	0.333 (0.032)	0.000 (0.000)	0.975	0.046	4.7	4.56
Tebuconazole	0.156 (0.007)	0.001 (0.000)	0.986	0.016	3.7	4.19
Cyproconazole	0.068 (0.002)	0.009 (0.002)	0.990	0.006	2.9	4.39
Epoxiconazole	0.171 (0.008)	0.001 (0.000)	0.990	0.015	3.7	4.33
Spiroxamine	0.126 (0.010)	0.040 (0.010)	0.991	0.010	2.5	4.42
Flurtamone	0.155 (0.013)	0.000 (0.000)	0.973	0.022	4.6	4.30
Thiodicarb	0.175 (0.007)	0.017 (0.007)	0.992	0.013	1.6	4.20
Prometryn	0.138 (0.005)	0.003 (0.005)	0.985	0.014	3.5	5.19
Dimethanamid	0.082 (0.003)	0.009 (0.003)	0.989	0.007	2.9	4.58
Chlorfenvinphos	0.485 (0.033)	0.000 (0.000)	0.972	0.070	3.8	4.56
Boscalid	0.438 (0.028)	0.000 (0.000)	0.979	0.054	4.9	5.10
DIA-d5	0.078 (0.002)	0.004 (0.001)	0.804	0.027	1.1	6.33

396 * Root-mean-square error.

397 + Information from the Pesticide Properties DataBase – PPDB (<http://sitem.herts.ac.uk/aeru/ppdb/en/atoz.htm>) and Ineris
 398 (<https://substances.ineris.fr/fr/>).

399 § Estimated with <https://www3.epa.gov/ceampubl/learn2model/part-two/onsite/estdiffusion-ext.html>

400

401 Table 2. k_e values and flow velocities either measured or calculated (with DIA-d5 desorption
 402 rates) from previous published works.

Conditions	References	k_e (d^{-1})	U_{measured} (cm s^{-1})	$U_{\text{estimated}}$ (cm s^{-1})
Lab 1. calibration	Fauvelle et al. (2012)	0.069	5-8	5.9
Lab 2. calibration	Lissalde et al. (2011)	0.057	2-3	3.8
Lab. 3 calibration	Mazzella et al. (2007)	0.047	2-3	2.5
<i>In situ</i>	Mazzella et al. (2010)	0.022	<1	0.5

403

Table 3. Sampling rates reported in some previous laboratory or field POCIS calibrations. Lab 1, 2 and 3 and *In situ* corresponds to the respective reference indicated in Table 2. Bias (%) between experimental and recalculated R_s are reported as well.

Chemicals	Sampling rates (mL.d ⁻¹)								Model parameters	
	Lab 1 (meas.)	Lab 1 (est.)	Lab 2 (meas.)	Lab 2 (est.)	Lab 3 (meas.)	Lab 3 (est.)	<i>In situ</i> (meas.)	<i>In situ</i> (est.)	<i>b</i>	<i>c</i>
Atrazine	263	363	228	310	239	262	59	131	0.074	0.011
Diuron	208	206	199	167	247	136	N/A	61	0.174	0.001
Acetochlor	348	319	241	270	225	227	N/A	111	0.088	0.010
Isoproturon	207	288	167	242	218	202	N/A	98	0.102	0.010
Metolachlor	305	355	182	298	N/A	250	N/A	121	0.082	0.008
Alachlor	325	303	205	248	N/A	203	N/A	93	0.112	0.003
Terbuthylazine	321	395	238	321	251	261	N/A	118	0.089	0.001
Dimethomorph	261	231	170	187	N/A	152	N/A	69	0.155	0.001
Mean	280	308	204	255	236	211	59	100	0.109	0.006
Standard dev.	54	65	30	56	14	48	N/A	25	0.036	0.005
									<i>b'</i>	<i>c'</i>
“Global” model output	-	249	-	214	-	183	-	94	0.100	0.019
Standard dev.	-	-	-	-	-	-	-	-	0.002	0.004
% Deviation from measured mean										
Bias* for “specific” models	-	+10%	-	+25%	-	-10%	-	+70%	-	-
Bias* for a “global” model	-	-11%	-	+5%	-	-23%	-	+59%	-	-

* Relative deviation between calculated mean R_s (with either specific or generic *b* and *c* parameters) and experimental mean R_s .

Acknowledgments

This study was financed by the Adour-Garonne French Water Agency. Authors would like to thank Gwilherm Jan and Sylvia Moreira from Inrae, and Julie Leblanc, Patrice Fondanèche and Karine Cleries from University of Limoges for technical and laboratory assistance.

References

- Ahrens, L., Daneshvar, A., Lau, A.E. and Kreuger, J. (2015) Characterization of five passive sampling devices for monitoring of pesticides in water. *Journal of Chromatography A* 1405(0), 1-11.
- Alvarez, D.A., Huckins, J.N., Petty, J.D., Jones-Lepp, T., Stuer-Lauridsen, F., Getting, D.T., Goddard, J.P., Gravell, A. and R. Greenwood, G.M.a.B.V. (2007) *Comprehensive Analytical Chemistry*, pp. 171-197, Elsevier.
- Alvarez, D.A., Petty, J.D., Huckins, J.N., Jones-Lepp, T.L., Getting, D.T., Goddard, J.P. and Manahan, S.E. (2004) Development of a passive, in situ, integrative sampler for hydrophilic organic contaminants in aquatic environments. *Environmental Toxicology and Chemistry* 23(7), 1640-1648.
- Bäuerlein, P.S., Mansell, J.E., ter Laak, T.L. and de Voogt, P. (2012) Sorption Behavior of Charged and Neutral Polar Organic Compounds on Solid Phase Extraction Materials: Which Functional Group Governs Sorption? *Environmental Science & Technology* 46(2), 954-961.
- Belles, A., Tapie, N., Pardon, P. and Budzinski, H. (2014) Development of the performance reference compound approach for the calibration of “polar organic chemical integrative sampler” (POCIS). *Analytical and Bioanalytical Chemistry* 406(4), 1131-1140.
- Bernard, M., Boutry, S., Guibal, R., Morin, S., Lissalde, S., Guibaud, G., Säut, M., Rebillard, J.-P. and Mazzella, N. (2023) Multivariate Tiered Approach To Highlight the Link between Large-Scale Integrated Pesticide Concentrations from Polar Organic Chemical Integrative Samplers and Watershed Land Uses. *Journal of Agricultural and Food Chemistry* 71(7), 3152-3163.
- Bernard, M., Boutry, S., Tapie, N., Budzinski, H. and Mazzella, N. (2022) Lab-scale investigation of the ability of Polar Organic Chemical Integrative Sampler to catch short pesticide contamination peaks. *Environmental Science and Pollution Research* 29(1), 40-50.
- Bonnaud, B., Mazzella, N., Boutet, P., Daval, A. and Miège, C. (2023) Calibration comparison between two passive samplers -o-DGT and POCIS- for 109 hydrophilic emerging and priority organic compounds. *Science of The Total Environment* 869, 161720.
- Bonnaud, B., Miège, C., Daval, A., Fauvelle, V. and Mazzella, N. (2022) Determination of diffusion coefficients in agarose and polyacrylamide gels for 112 organic chemicals for passive sampling by organic Diffusive Gradients in Thin films (o-DGT). *Environmental Science and Pollution Research* 29(17), 25799-25809.
- Booij, K. and Chen, S. (2018) Review of atrazine sampling by polar organic chemical integrative samplers and Chemcatcher. *Environmental Toxicology and Chemistry* 37(7), 1786-1798.
- Booij, K., Chen, S. and Trask, J.R. (2020) POCIS Calibration for Organic Compound Sampling in Small Headwater Streams. *Environmental Toxicology and Chemistry* 39(7), 1334-1342.
- Booij, K., Maarsen, N.L., Theeuwen, M. and van Bommel, R. (2017) A method to account for the effect of hydrodynamics on polar organic compound uptake by passive samplers. *Environmental Toxicology and Chemistry* 36(6), 1517-1524.
- Booij, K. and Smedes, F. (2010) An Improved Method for Estimating in Situ Sampling Rates of Nonpolar Passive Samplers. *Environmental Science & Technology* 44(17), 6789-6794.
- Buzier, R., Guibal, R., Lissalde, S. and Guibaud, G. (2019) Limitation of flow effect on passive sampling accuracy using POCIS with the PRC approach or o-DGT: A pilot-scale evaluation for pharmaceutical compounds. *Chemosphere* 222, 628-636.
- Challis, J.K., Hanson, M.L. and Wong, C.S. (2016) Development and Calibration of an Organic-Diffusive Gradients in Thin Films Aquatic Passive Sampler for a Diverse Suite of Polar Organic Contaminants. *Analytical Chemistry* 88(21), 10583-10591.

Dalton, R.L., Pick, F.R., Boutin, C. and Saleem, A. (2014) Atrazine contamination at the watershed scale and environmental factors affecting sampling rates of the polar organic chemical integrative sampler (POCIS). *Environmental Pollution* 189, 134-142.

Fauvelle, V., Kaserzon, S.L., Montero, N., Lissalde, S., Allan, I.J., Mills, G., Mazzella, N., Mueller, J.F. and Booi, K. (2017a) Dealing with Flow Effects on the Uptake of Polar Compounds by Passive Samplers. *Environmental Science & Technology* 51, 2536–2537.

Fauvelle, V., Mazzella, N., Belles, A., Moreira, A., Allan, I.J. and Budzinski, H. (2014) Optimization of the polar organic chemical integrative sampler for the sampling of acidic and polar herbicides. *Analytical and Bioanalytical Chemistry* 406(13), 3191-3199.

Fauvelle, V., Mazzella, N., Delmas, F., Madarassou, K., Eon, M. and Budzinski, H. (2012) Use of Mixed-Mode Ion Exchange Sorbent for the Passive Sampling of Organic Acids by Polar Organic Chemical Integrative Sampler (POCIS). *Environmental Science & Technology* 46(24), 13344-13353.

Fauvelle, V., Montero, N., Mueller, J.F., Banks, A., Mazzella, N. and Kaserzon, S.L. (2017b) Glyphosate and AMPA passive sampling in freshwater using a microporous polyethylene diffusion sampler. *Chemosphere* 188, 241-248.

Guibal, R., Buzier, R., Lissalde, S. and Guibaud, G. (2019) Adaptation of diffusive gradients in thin films technique to sample organic pollutants in the environment: An overview of o-DGT passive samplers. *Science of The Total Environment* 693, 133537.

Guibal, R., Lissalde, S. and Guibaud, G. (2020) Experimental Estimation of 44 Pharmaceutical Polar Organic Chemical Integrative Sampler Sampling Rates in an Artificial River under Various Flow Conditions. *Environmental Toxicology and Chemistry* 39(6), 1186-1195.

Harman, C., Allan, I.J. and B auerlein, P.S. (2011) The Challenge of Exposure Correction for Polar Passive Samplers—The PRC and the POCIS. *Environmental Science & Technology* 45(21), 9120-9121.

Lissalde, S., Mazzella, N., Fauvelle, V., Delmas, F., Mazellier, P. and Legube, B. (2011) Liquid chromatography coupled with tandem mass spectrometry method for thirty-three pesticides in natural water and comparison of performance between classical solid phase extraction and passive sampling approaches. *J. Chromatogr. A* 1218, 1492-1502.

Lissalde, S., Mazzella, N. and Mazellier, P. (2014) Polar organic chemical integrative samplers for pesticides monitoring: Impacts of field exposure conditions. *Science of the Total Environment* 488-489, 188-196.

Mazzella, N., Dubernet, J.-F. and Delmas, F. (2007) Determination of kinetic and equilibrium regimes in the operation of polar organic chemical integrative samplers: Application to the passive sampling of the polar herbicides in aquatic environments. *J. Chromatogr. A* 1154(1-2), 42-51.

Mazzella, N., Lissalde, S., Moreira, S., Delmas, F., Mazellier, P. and Huckins, J.N. (2010) Evaluation of the Use of Performance Reference Compounds in an Oasis-HLB Adsorbent Based Passive Sampler for Improving Water Concentration Estimates of Polar Herbicides in Freshwater. *Environmental Science & Technology* 44(5), 1713-1719.

Morin, N., Camilleri, J., Cren-Oliv e, C., Coquery, M. and Mi ge, C. (2013) Determination of uptake kinetics and sampling rates for 56 organic micropollutants using “pharmaceutical” POCIS. *Talanta* 109(0), 61-73.

Morin, N.A.O., Mazzella, N., Arp, H.P.H., Randon, J., Camilleri, J., Wiest, L., Coquery, M. and Mi ge, C. (2018) Kinetic accumulation processes and models for 43 micropollutants in “pharmaceutical” POCIS. *Science of The Total Environment* 615, 197-207.

Poulier, G., Lissalde, S., Charriau, A., Buzier, R., Delmas, F., Gery, K., Moreira, A., Guibaud, G. and Mazzella, N. (2014) Can POCIS be used in Water Framework Directive (2000/60/EC)

monitoring networks? A study focusing on pesticides in a French agricultural watershed. *Sci Total Environ* 497-498, 282-292.

Söderström, H., Lindberg, R.H. and Fick, J. (2009) Strategies for monitoring the emerging polar organic contaminants in water with emphasis on integrative passive sampling. *Journal of Chromatography A* 1216(3), 623-630.

Vermeirssen, E.L.M., Dietschweiler, C., Escher, B.I., van der Voet, J. and Hollender, J. (2012) Transfer Kinetics of Polar Organic Compounds over Polyethersulfone Membranes in the Passive Samplers Pocis and Chemcatcher. *Environmental Science & Technology* 46(12), 6759-6766.

Vrana, B., Mills, G.A., Allan, I.J., Dominiak, E., Svensson, K., Knutsson, J., Morrison, G. and Greenwood, R. (2005) Passive sampling techniques for monitoring pollutants in water. *Trends in Analytical Chemistry* 24, 845-868.

Supplementary material

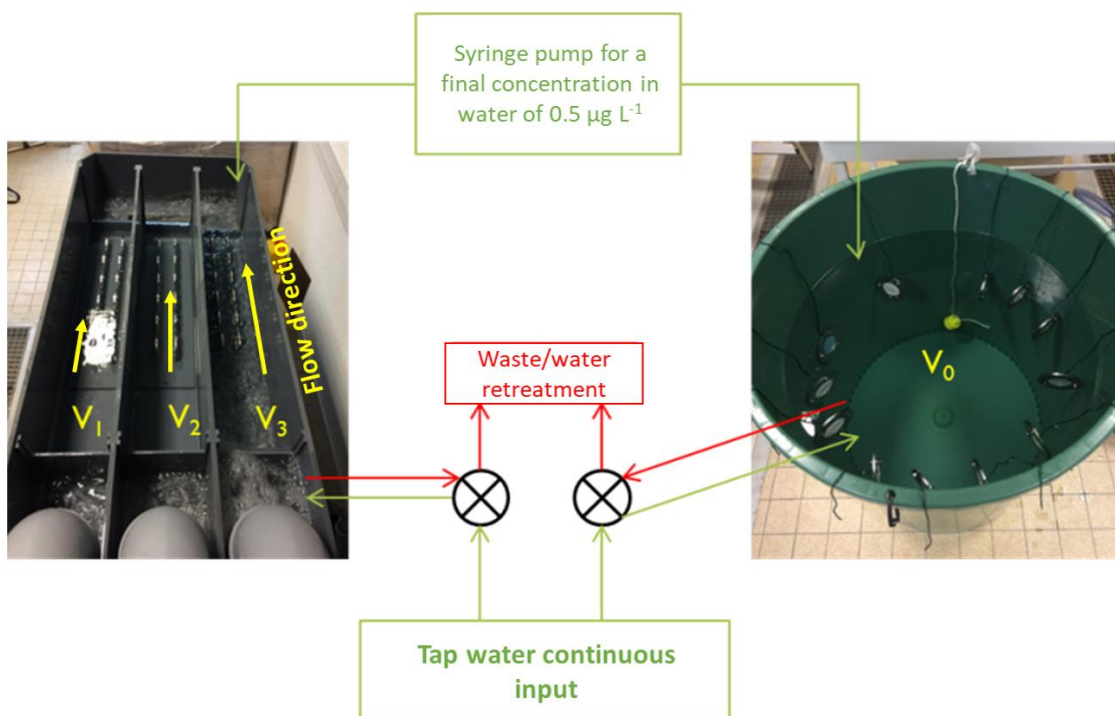


Figure S 1. Schema of the system used to calibrate POCIS HLB at different flow velocities.

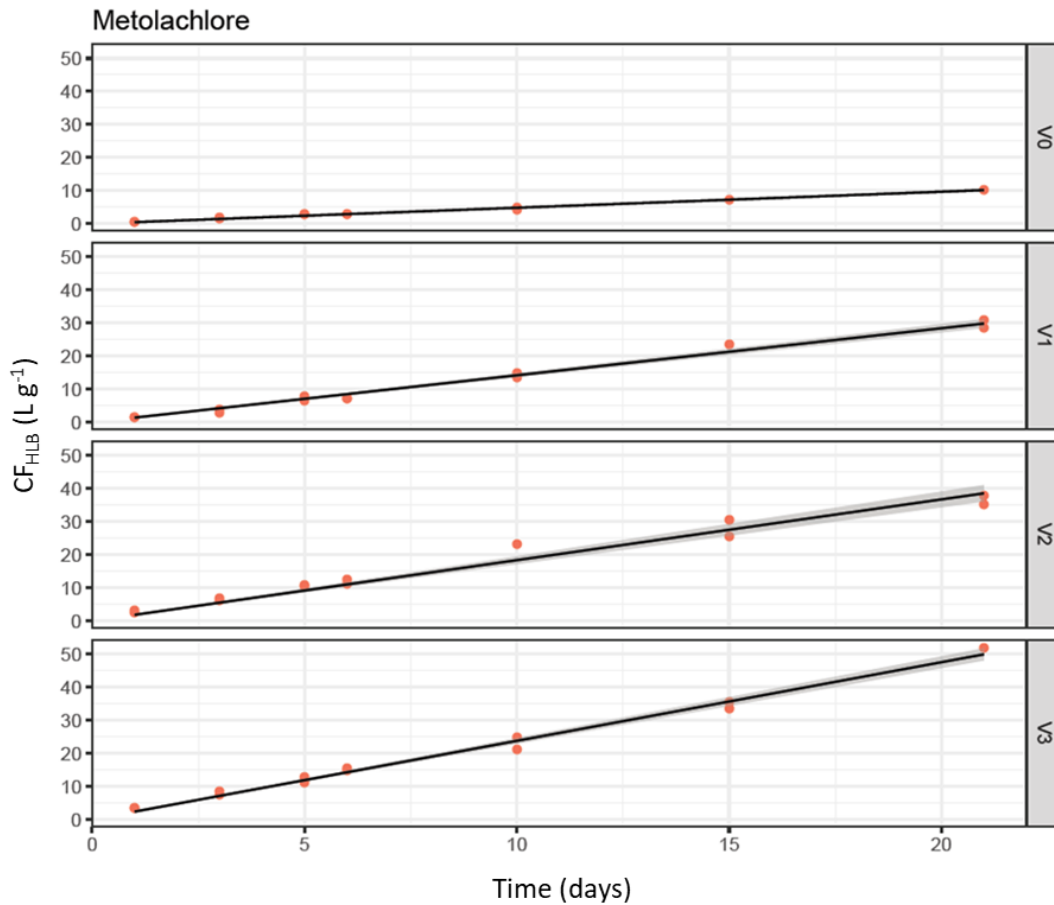


Figure S 2. Example of metolachlor linear uptake obtained during laboratory calibration of POCIS and associated with the four flow velocities (V0 to V3).

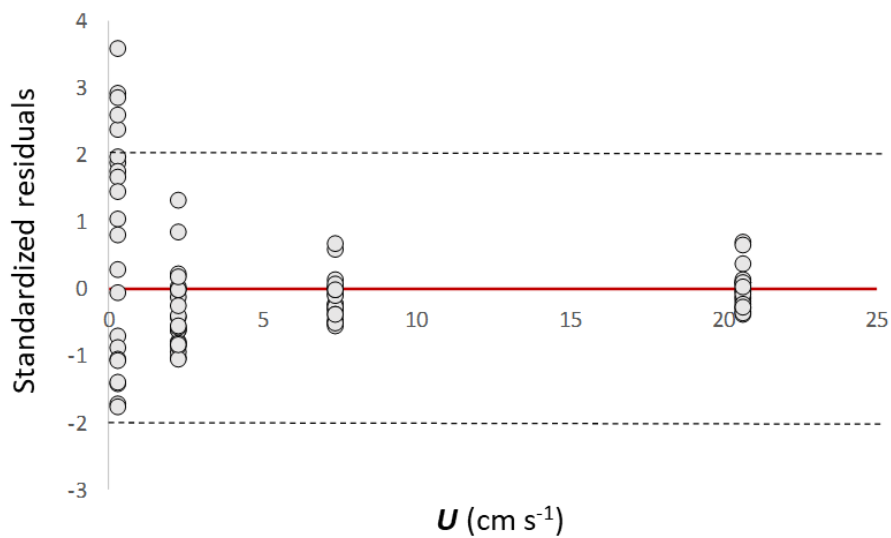


Figure S 3. Plotting of residuals for the fitting of Equation 6. The grey horizontal dashed lines correspond to the 95 % confidence interval limits.

Table S 1. 2-way ANOVA results for the likely effects of the log K_{ow} or D_w factors on the coefficients b and c derived from the calibrated chemicals (Table 1).

Coefficients (b) :

Factors	Values	Standard error	t	p-value	Lower limit (95%)	Higher limit (95%)
log K_{ow}	0.373	0.244	1.527	0.141	-0.134	0.88
D_w	0.137	0.244	0.56	0.581	-0.37	0.644

Coefficients (c) :

Factors	Values	Standard error	t	p-value	Lower limit (95%)	Higher limit (95%)
log K_{ow}	-0.6	0.205	-2.919	0.008	-1.026	-0.174
D_w	0.007	0.205	0.036	0.972	-0.419	0.433

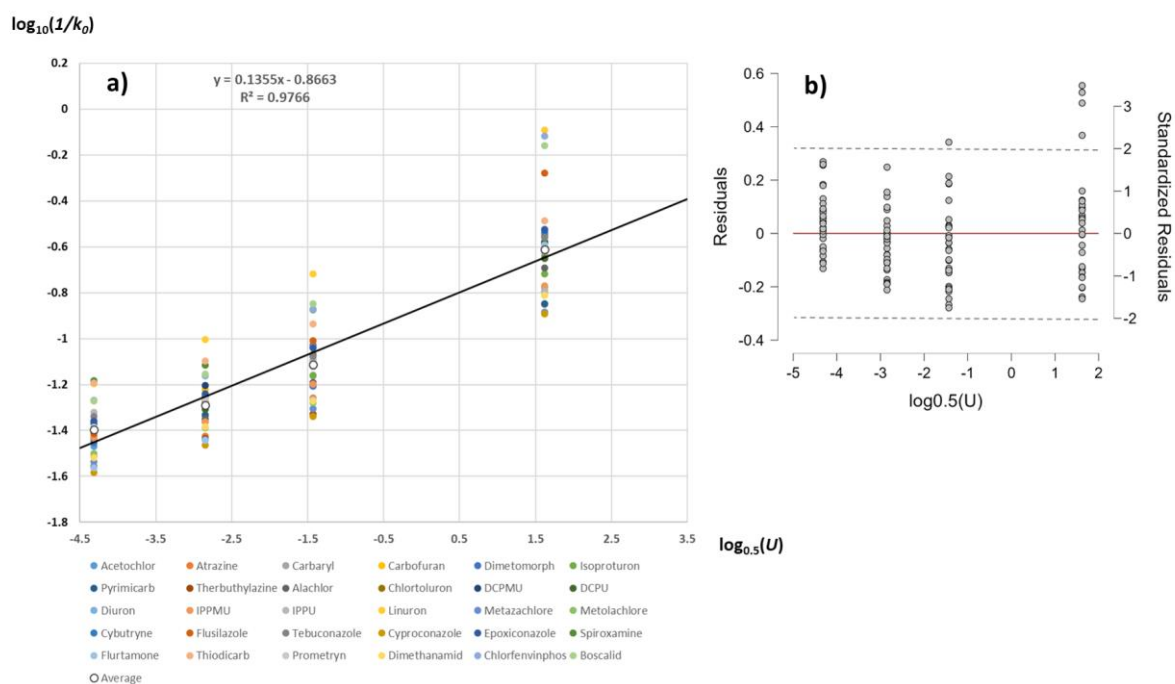


Figure S 4. Logarithmic transformation (Equation 8) of x and y values (a), and corresponding plotting of residuals (b). The grey horizontal dashed lines (b panel) correspond to the 95 % confidence interval limits.

Table S 2. F-test results for the fitting of Equation 8.

	Sum of Squares	df	Mean Square	F	p
$X=\log_{0.5}(U)$	10.61	1	10.6075	416	< .001
Residuals	3.01	118	0.0255		

Note. Type 3 sum of squares.